IOP Publishing Journal of Physics D: Applied Physics
J. Phys. D: Appl. Phys. **50** (2017) 405110 (6pp) https://doi.org/10.1088/1361-6463/aa82f4

Ultrathin microwave metamaterial absorber utilizing embedded resistors

Young Ju Kim[1], Ji Sub Hwang[1], Young Joon Yoo[1], Bui Xuan Khuyen[1], Joo Yull Rhee[2], Xianfeng Chen[3] and YoungPak Lee[1]

[1] Department of Physics, Quantum Photonic Science Research Center and RINS, Hanyang University, Seoul, 04763, Republic of Korea
[2] Sungkyunkwan University, Suwon, Republic of Korea
[3] Shanghai Jiaotong University, Shanghai, People's Republic of China

E-mail: yplee@hanyang.ac.kr

Received 22 April 2017, revised 11 July 2017
Accepted for publication 28 July 2017
Published 13 September 2017

Abstract

We numerically and experimentally studied an ultrathin and broadband perfect absorber by enhancing the bandwidth with embedded resistors into the metamaterial structure, which is easy to fabricate in order to lower the Q-factor and by using multiple resonances with the patches of different sizes. We analyze the absorption mechanism in terms of the impedance matching with the free space and through the distribution of surface current at each resonance frequency. The magnetic field, induced by the antiparallel surface currents, is formed strongly in the direction opposite to the incident electromagnetic wave, to cancel the incident wave, leading to the perfect absorption. The corresponding experimental absorption was found to be higher than 97% in 0.88–3.15 GHz. The agreement between measurement and simulation was good. The aspects of our proposed structure can be applied to future electronic devices, for example, advanced noise-suppression sheets in the microwave regime.

Keywords: metamaterials, perfect absorption, microwave

(Some figures may appear in colour only in the online journal)

1. Introduction

Artificially-created metamaterials (MMs), which are composed of periodically-arranged unit cells with adjustable electric permittivity and magnetic permeability, have enabled the production of electromagnetic (EM) materials with properties not observed in nature, such as extraordinary optical transmission [1] and negative refraction index [2]. Because of their remarkable properties, many researchers have applied them to diverse applications, for example, invisibility cloaks [3], radomes [4], amplifiers [5] and absorbers [6] from radio wave [7] to visible light [8].

Since a MM perfect absorber (PA) for various applications was introduced by Landy *et al* [9], a number of the optimized MMPAs have been reported for diverse application areas such as photodetectors [10], solar cells [11], bolometers [12] and sensors [13]. MMPAs are generally composed of three layers: a patterned metallic layer, a dielectric layer and a continuous metallic layer. The continuous metallic layer plays a role of stemming the EM wave, and the optimized MMPA attains the absorption properties through dielectric loss and perfect impedance matching at the magnetic resonance [14]. In comparison with the well-known absorbers like ferrite, Jaumann absorber [15] and Salisbury screen absorber [16], the MMPA has a virtue, a high absorption in a thin thickness. Yoo *et al* reported an MMPA with an ultrathin thickness ($\lambda/62$), with respect to the wavelength of operation, based on a snake-shaped structure [17]. Recently, in the VHF (very-high-frequency) radio band (30–300 MHz), Khuyen *et al* proposed and demonstrated ultrathin MMPA with a thickness of only $\lambda/816$ [18]. However, there are few studies on the thin MMPAs to present wide-band high absorption, and this remains a challenge to be overcome.

In this work, we realize the ultrathin and ultrabroad microwave MMPA utilizing resonators of different sizes and embedded resistors, which are easy to be fabricated in MM. It should be noted that, in order to achieve the wide-band absorber, we apply the concept of embedded resistors, which

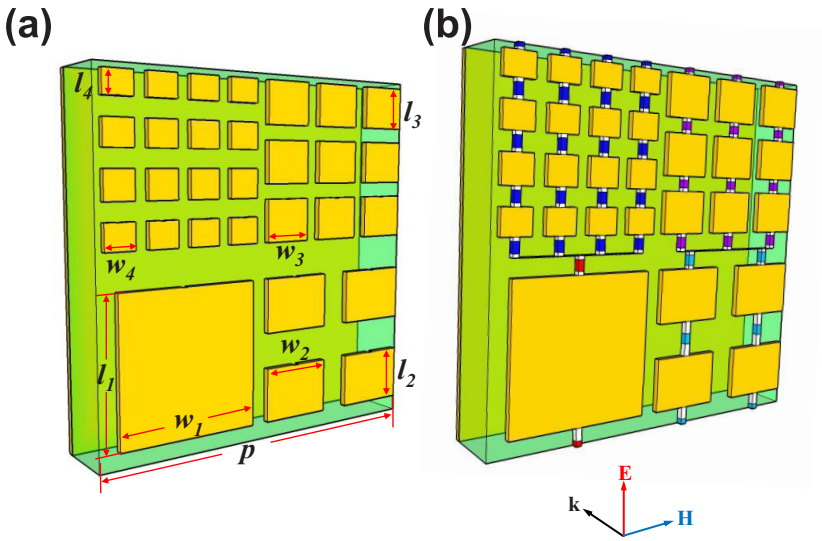

Figure 1. (a) Schematic diagram of the MMPA (a) without and (b) with embedded resistors.

expand the operating bandwidth because of the low-quality factor. Actually, the MMPA by using resistors has been already studied. Ye *et al* suggested an ultra-broadband MMPA with a lumped resistor [19]. However, it can be verified that it is thick because it is not a flat MM. Dung *et al* proposed a planar MMPA with an embedded resistor [20]. The proposed structure is similar to ours, but we exploit the quadruple resonators. It is confirmed that the structure in [20] is very thin compared to the operating wavelength, because of the MMPA whose structure connecting the resistors is optimized. The absorption mechanism can be interpreted by using the surface-averaged current-density method [21], but we interpret it as utilizing magnetic resonance through the surface current distribution. Both experiment and simulation were performed, and it is found that the results of simulation are in good accordance with those of the experiment.

2. Design, results and discussion

A numerical structure, simulated by using finite-element-method software, CST Microwave Studio, is used to estimate the properties of proposed MMPA. In simulation, the boundary condition was set: the *E-H* fields and the direction of propagation (k) made the x-y plane and the z direction, respectively. Figure 1 shows the unit cell of MMPA without and with embedded resistors. The unit cell is mainly composed of three layers. A dielectric layer is located between metallic patterns at the front and metallic plane at the bottom. The unit cell contains rectangular metallic patches with different sizes and is repeated with a periodicity of $p = 400$ mm. In the *E-H* plane, the optimum values for the lengths of patches with different sizes come to be $l_1 = 80$, $l_2 = 70$, $l_3 = 55$ and $l_4 = 35$ mm, and the corresponding widths become $w_1 = 180$, $w_2 = 90$, $w_3 = 60$ and $w_4 = 45$ mm. In order to absorb the EM wave in 1–3 GHz, the largest patch with resistors was designed to have absorption over 99% at 1 GHz, and then we designed the other optimized patches with periods of 1/2, 1/3, and 1/4 of the largest patch so that they achieve the goal together. The proposed structure includes metallic layers (0.036 mm thick) and dielectric layers (0.8 mm thick) in the k direction. In figure 1(b), the embedded resistors of 150, 75, 22 and 19 kΩ were connected to the metallic patches, which are arranged so that the surface current is able to flow parallel to the electric-field direction of incident EM wave. The resistors (red) connected above and below the largest patch are 150 kΩ, and the resistors (cyan) connected between the second largest patches are 75 kΩ. The resistors (violet) for the third largest patches are 22 kΩ, and the resistors (blue) between the smallest patches are 19 kΩ. These resistance values are obtained by simulating the optimized resistance for each patch. The employed metal was copper with a conductivity of 5.8×10^7 S m^{-1}, and the selected dielectric was FR-4 with a dielectric constant of 4.3 and a loss tangent of 0.025. The absorption is calculated as $A(\omega) = 1 - R(\omega) - T(\omega) = 1 - |S_{11}(\omega)|^2 - |S_{21}(\omega)|^2$. $A(\omega)$, $R(\omega)$ and $T(\omega)$ become absorption, reflection and transmission, respectively, and the scattering parameters of reflection and transmission come to be $S_{11}(\omega)$ and $S_{21}(\omega)$, respectively, in simulation. The absorption was defined as $A(\omega) = 1 - R(\omega) = 1 - |S_{11}(\omega)|^2$, because a metal plate was located at the bottom in order to prevent the EM-wave transmission as in the conventional MMPAs.

The simulated absorption spectrum of the proposed structure without embedded resistors [figure 1(a)], which is designed in order to demonstrate multi-band absorption, is illustrated in figure 2(a) for a frequency range of 0.5–3.5 GHz. We can clearly see quadruple absorption peaks at 1.01, 1.28, 1.96 and 3.01 GHz with absorption of 28.7%, 40.8%, 48.3% and 11.2%, respectively. In addition, weak absorption peaks with 7.1% and 2.9% at 1.2 and 2.79 GHz, respectively, are observed. The absorption is not high for the structure without embedded resistors, because this structure is designed in order to have a high absorption in the broadband only when the resistors are connected. The ratios (t/λ) of dielectric thickness with respect to resonance wavelength are 1/371, 1/293, 1/191 and 1/125 at 1.01, 1.28, 1.96 and 3.01 GHz, respectively, and these small values indicate that the layer is

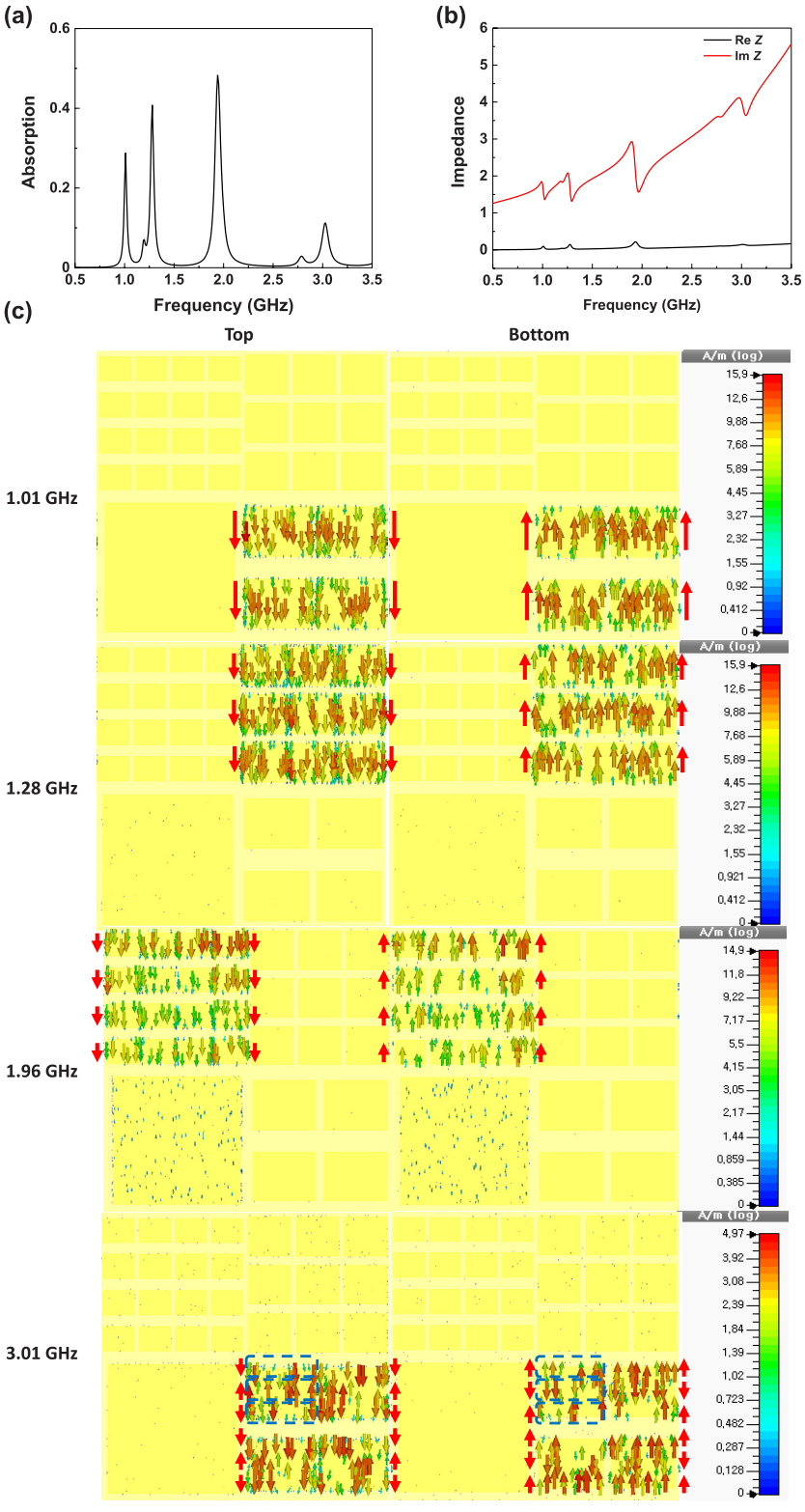

Figure 2. (a) Simulated absorption and (b) effective impedance spectrum of the proposed MMPA without embedded resistors. (c) Distribution of the induced surface currents in the metallic pattern (left) and the continuous metallic plane (right) at 1.01, 1.28, 1.96 and 3.01 GHz.

very thin. Based on the conventional free-space impedance-matching theory by adjusting the electric permittivity $\epsilon(\omega)$ and the magnetic permeability $\mu(\omega)$ at the absorption frequency, the absorption property can be explained [impedance $Z(\omega) = \sqrt{\mu(\omega)/\epsilon(\omega)} = 1$]. The computable effective impedance equation in terms of the scattering parameters turns out to be [22]

$$Z(\omega) = \sqrt{\frac{(1+S_{11})^2 - {S_{21}}^2}{(1-S_{11})^2 - {S_{21}}^2}}. \quad (1)$$

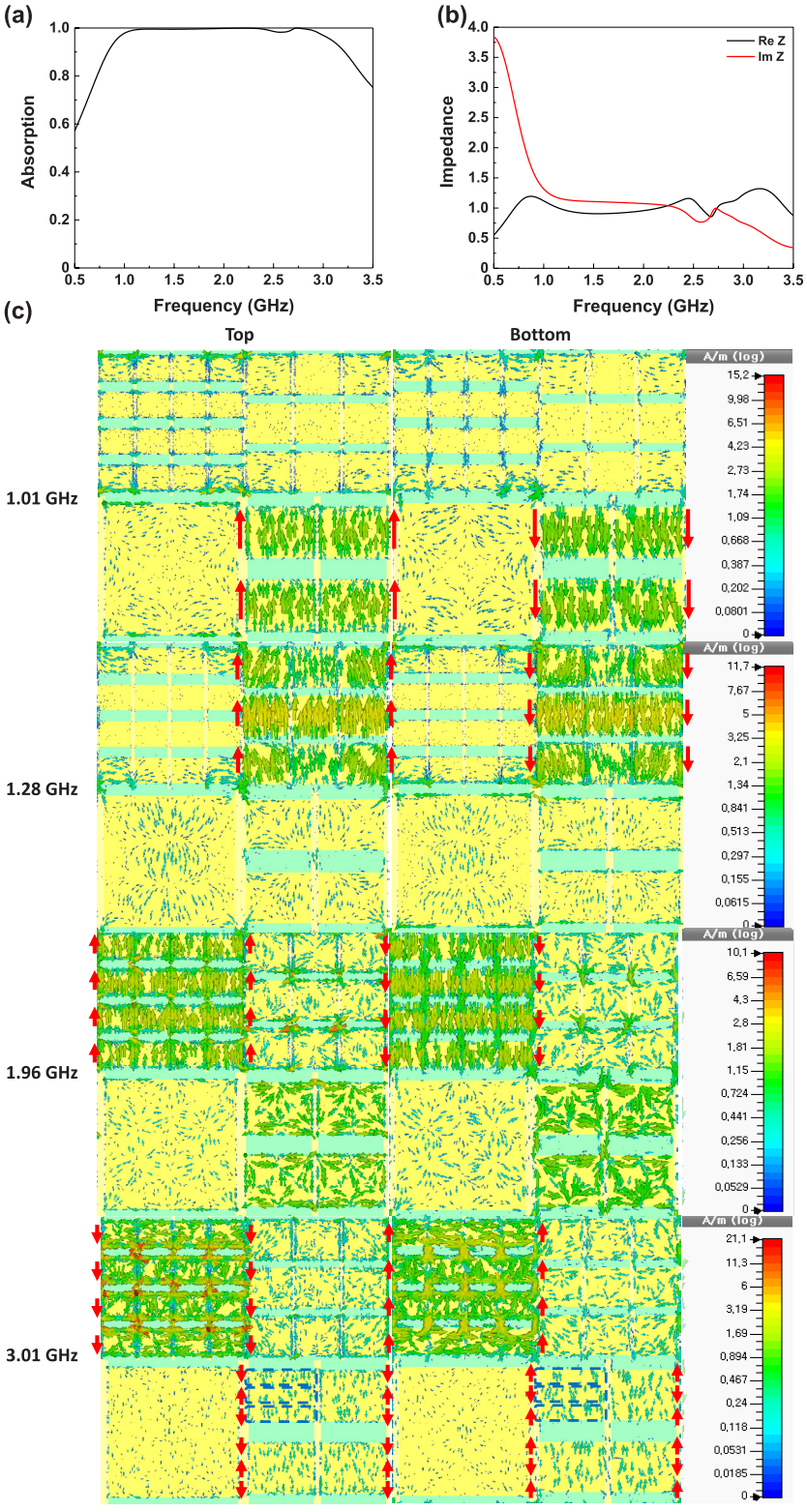

Figure 3. (a) Simulated absorption and (b) effective impedance spectrum of the proposed MMPA with embedded resistors. (c) Distribution of the induced surface currents in the metallic pattern (left) and the continuous metallic plane (right) at 1.01, 1.28, 1.96 and 3.01 GHz.

As shown in figure 2(b), both calculated real and imaginary parts of the relative impedance are illustrated. In the real part of relative impedance, a small signature appears at the resonance frequencies. The imaginary part of relative impedance comes to be approximately 1, not 0, at the absorption frequencies, except 3.01 GHz. Figure 2(c) shows the distribution of the antiparallel surface currents on the front and the back metallic layers at the absorption frequencies. The absorption occurs by the antiparallel surface currents of the second-largest rectangular resonators (the bottom right pattern) at 1.01 GHz. It can be also observed that those cause the absorption at 3.01 GHz as well as 1.01 GHz, because this

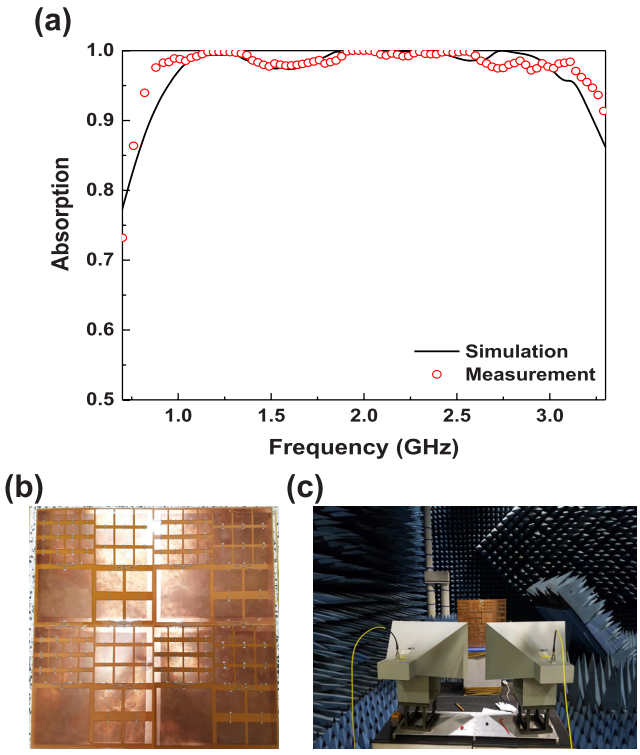

Figure 4. (a) Simulated and measured absorption spectra for the proposed structure. Photographs of (b) the fabricated samples with connecting resistors and (c) the measurement configuration.

is the third-harmonic magnetic resonance of that at 1.01 GHz [23]. The absorption at 1.28 GHz is analyzed to be due to the third-largest rectangular resonators (the upper right pattern), and that at 1.96 GHz due to the smallest rectangles (the upper left pattern). Those of the largest rectangular resonator (the bottom left pattern) appear at 1.2 and 2.79 GHz. The third- and the seventh-harmonic magnetic resonances are formed at these frequencies. By elucidating the surface-current distribution, it can be confirmed that the absorption is realized by the magnetic resonances.

The simulated absorption spectrum of proposed structure with embedded resistors (figure 1(b)), which is designed in order to demonstrate broadband absorber, plotted in figure 3(a) from 0.5 to 3.5 GHz. The simulated absorption band over 97% is from 0.99 to 3.03 GHz. In figure 3(b), both real and imaginary parts of the relative impedance get close to 1 in this frequency range unlike the structure without embedded resistors. Therefore, there is no reflection wave in the MMPA. Figure 3(c) presents the distribution of the antiparallel surface currents on the front and the back metallic layers at the absorption frequencies. As aforementioned, the absorption occurs by the antiparallel surface currents of the second-largest rectangular resonators (the bottom right pattern) at 1.01 GHz, and the absorption at 1.28 and 1.96 GHz by the antiparallel surface currents of the third-largest rectangles (the upper right pattern) and the smallest rectangles (the upper left pattern), respectively. However, the antiparallel surface currents of the second-largest rectangles and the smallest rectangles work simultaneously at 3.01 GHz unlike the structure without embedded resistors. Hence, the absorption was also improved at this frequency.

In the generic equivalent RLC circuit, the quality factor in terms of the losses in the metallic conductor can be defined as [24]

$$Q_c = \omega_0 \frac{L}{R}. \tag{2}$$

Here, ω_0, L and R is the angular resonant frequency, the inductance and the capacitance of circuit [$\omega_0 = \sqrt{LC}$]. The operating bandwidth is given by

$$BW = \frac{f_0}{Q_c} = \frac{R}{2\pi L} \tag{3}$$

where f_0 is the resonance frequency, which is defined by $f_0 = 1/2\pi\sqrt{LC}$. The absorption peaks are connected in order to form a wide band due to the fact the resistance plays a role in expanding the operating bandwidth.

We have measured the absorption spectrum in the frequency range of 0.7–3.3 GHz in order to compare the simulation results in figure 4. The samples were fabricated by the conventional printed-circuit-board process with a size of $80 \times 80\,\mathrm{cm}^2$ and the surface mounting technique with solder (figure 4(b)). The reflection were measured in a microwave anechoic chamber using a Hewlett Packard E8362B network analyzer, and the distance between two antennas and the sample was properly set in order to avoid the near-field effects. The illuminating and the receiving horn antennas were each tilted at an angle of 5° about the normal direction of sample to prevent the interference effect between incident and reflected waves (as shown figure 4(c)). Therefore, the measured scattering parameter of reflection is $S_{21}(\omega)$, and the measured absorption is defined as $A(\omega) = 1 - |S_{21}(\omega)|^2$. The measured absorption of the fabricated sample is in good agreement with the simulated one as in figure 4(a). In order to compare the measurement at an incident angle of 5°, the corresponding simulation for an incident angle of 5° was performed. The simulated absorption band over 97% emerges in 0.99–3.03 GHz, and the measured absorption turns out to be over 97% in 0.88–3.15 GHz. The scattering from defects in the fabricated sample and the scattering between the two horn antennas could cause the subtle distinction between simulated and measured absorption spectra, and the two most significant reasons for broader frequency bandwidth in the experimental results are the difference between real and assumed values of the employed FR4 dielectric loss and the embedded resistor.

3. Conclusions

In conclusion, the absorption performance for a proposed ultrathin MMPA was analyzed by simulation and experiment in 0.5–3.5 GHz. By manipulating the magnetic resonance in resonators of different sizes and embedded resistors, which are easy to be fabricated in MM, the dielectric layer comes to be efficiently thin, 0.8 mm (corresponding to $\lambda/371$), at 1.01 GHz, and the broadband absorption over 97% is obtained at the same time. In addition, the absorption mechanism was demonstrated at the resonance frequencies through comparing with the sample without embedded resistors. The measurements were performed, based on the simulation results

in 0.7–3.3 GHz, and the agreement between measurement and simulation was achieved. Our proposed structure can be applied to future electronic devices, such as advanced noise-suppression sheets, in the microwave regime.

Acknowledgments

This work was supported by the Institute for Information & Communication Technology Promotion (IITP) grant funded by the Korean government (MSIT) (2013-0-00375) and by the NRF funded by MSIT, Korea (No. 2017R1A2B4003916).

References

[1] Navarro-Cia M, Beruete M, Campillo I and Sorolla M 2011 *Phys. Rev.* B **83** 115112
[2] Shalaev V M 2007 *Nat. Photon.* **1** 41
[3] Schurig D, Mock J J, Justice B J, Cummer S A, Pendry J B, Starr A F and Smith D R 2006 *Science* **314** 977
[4] Chen H, Wu B-I, Ran L, Grzegorczyk T M and Kong J A 2006 *Appl. Phys. Lett.* **89** 053509
[5] Castellanos-Beltran M A, Irwin K D, Hilton G C, Vale L R and Lehnert K W 2008 *Nat. Phys.* **4** 929
[6] Tao H, Landy N I, Bingham C M, Zhang X, Averitt R D and Padilla W J 2008 *Opt. Express* **16** 7181
[7] Ghamsari B G, Abrahams J, Remillard S and Anlage S M 2013 *Appl. Phys. Lett.* **102** 013503
[8] Burgos S P, Waele R D, Polman A and Atwater H A 2010 *Nat. Mater.* **9** 407
[9] Landy N I, Sajuyigbe S, Mock J J, Smith D R and Padilla W J 2008 *Phys. Rev. Lett.* **100** 207402
[10] Song S, Chen Q, Jin L and Sun F 2013 *Nanoscale* **5** 9615
[11] Wang Y, Sun T, Paudel T, Zhang Y, Ren Z and Kempa K 2012 *Nano Lett.* **12** 440
[12] Grant J, Escorcia-Carranza I, Li C, McCrindle I J H, Gough J and Cumming D R S 2013 *Laser Photon. Rev.* **7** 1043
[13] Liu N, Mesch M, Weiss T, Hentschel M and Giessen H 2010 *Nano Lett.* **10** 2342
[14] Zhou J, Economon E N, Koschny T and Soukoulis C M 2006 *Opt. Lett.* **31** 3620
[15] Munk B A, Munk P and Pryor J 2007 *IEEE Trans. Antennas Propag.* **55** 186
[16] Fante R L and McCormack M T 1988 *IEEE Trans. Antennas Propag.* **36** 1443
[17] Yoo Y J, Zheng H Y, Kim Y J, Rhee J Y, Kang J-H, Kim K W, Cheong H, Kim Y H and Lee Y P 2014 *Appl. Phys. Lett.* **105** 041902
[18] Khuyen B X, Tung B S, Yoo Y J, Kim Y J, Kim K W, Chen L-Y, Lam V D and Lee Y P 2017 *Sci. Rep.* **7** 45151
[19] Ye D, Wang Z, Xu K, Li H, Huangfu J, Wang Z and Ran L 2013 *Phys. Rev. Lett.* **111** 187402
[20] Dung N V *et al* 2015 *J. Opt.* **17** 045105
[21] Ra'di Y, Simovski C R and Tretyakov S A 2015 *Phys. Rev. Appl.* **3** 37001
[22] Smith D R, Vier D C, Koschny T and Soukoulis C M 2005 *Phys. Rev.* E **71** 036617
[23] Yoo Y J, Kim Y J, Tuong P V, Rhee J Y, Kim K W, Jang W H, Kim Y H, Cheong H and Lee Y P 2013 *Opt. Express* **21** 32484
[24] Bilotti F, Toscano A, Vegni L, Aydin K, Alici K B and Ozbay E 2007 *IEEE Trans. Microw. Theory Tech.* **55** 2865